Search for invisible Higgs boson decays with vector boson fusion signatures with the ATLAS detector using an integrated luminosity of 139 fb^{-1}

David Casado

- Direct search for the decay of the Higgs boson produced via the vector boson fusion (VBF) process into invisible particles ($\chi\bar{\chi}$)

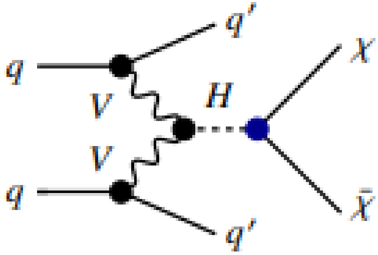

(a) Signal process

- Model under consideration where the Higgs boson decay into a pair of weakly interacting massive particles (WIMPs), which are candidates to explain the existence of dark matter (DM)

- The experimental signature of the VBF production process is a pair of energetic quark-induced jets with a wide gap in pseudorapidity Δn_{jj} resulting in large invariant masses m_{jj} of the two jets with the highest transverse momenta p_T in the event.
- Direct searches for invisible Higgs boson decays look for an excess of events over Standard Model expectations in various final states: ggF, VBF, and associated production with W, Z or t pairs
- Events with no leptons, not back to back jets

- Absence of an excess is interpreted as an upper limit on B_{inv}. Expectation for the branching fraction of invisible decays B_{inv} from the Standard Model (SM) is 0.12 %
- The extracted signal yield from a fit is used to determine an upper limit on B_{inv}.
- Previous ATLAS paper the selection criteria on m_{jj}, $\Delta\eta_{jj}$ and the azimuthal angular difference between the two highest-p_T jets $\Delta\phi_{jj}$ are relaxed while the E_T^{miss} requirement is slightly increased.
- Also Events with three or four jets are considered in this analysis differing from the previous one

ATLAS Detector

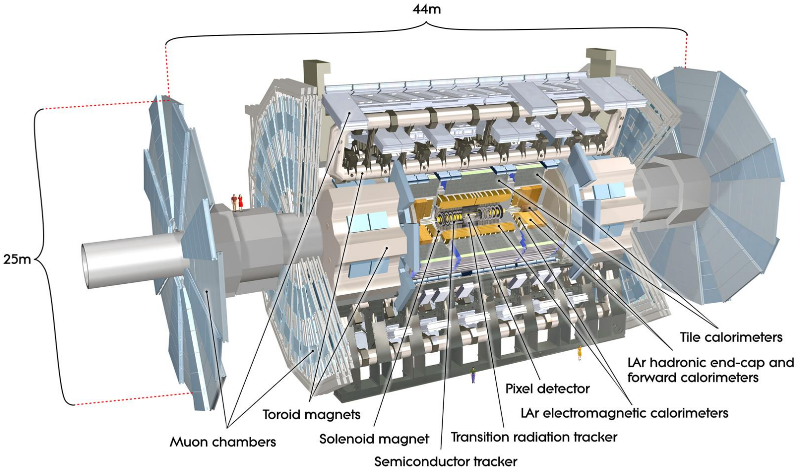

Data and Triggers

- D Proton-proton collisions at $\sqrt{s} = 13$ TeV collected by ATLAS in 2015–2018. A total integrated luminosity of 139 fb^{-1} is used, with the uncertainty of 1.7 %
- T Recorded with E_T^{miss} triggers
- Triggers are used for keeping the data we are searching for with an algorithm

Event Simulation

Simulated samples are used to model both the signal and background processes.

1 V+jets and VV+jets

- $Z \rightarrow vv$ $W \rightarrow lv$ $Z \rightarrow ll$ (l = e or μ)
- Split into two components. Order in the coupling constant α_{EW}
- Strong $\Rightarrow$ Order α_{EW}^2 diagrams

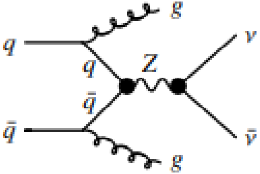

(b) Example diagram for the strong Z+jets background process

Event Simulation

Simulated samples are used to model both the signal and background processes.

- Electroweak $\Rightarrow$ Order α_{EW}^4 diagrams
  - VBF diagrams
  - Semileptonic diboson diagrams
- Negligible α_{EW}^3. Data driven with use of MC generators to check.

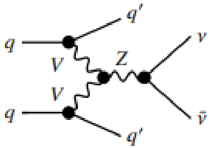

(c) Example diagram for the electroweak VBF Z+jets background process

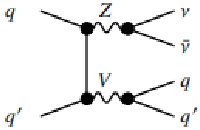

(d) Example diagram for the electroweak diboson process

2 $t\bar{t}, tW$ and sigle top. Modelled with MC generators

3 QCD multijet. Data driven with the use of MC generators for check.

4 ggF Higgs, VBF Higgs, VH Higgs. Modelled with MC generators

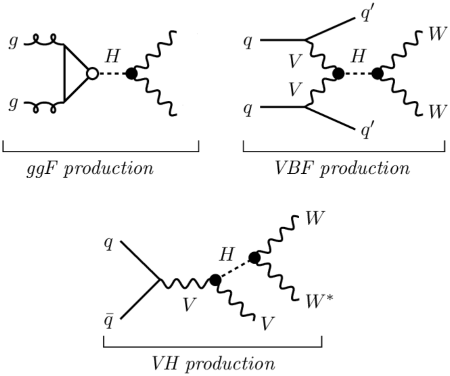

- Electrons
  - $p_T > 4.5$GeV, $|\eta| <2.47$ and loose identification
- Muons
  - $p_T > 4$GeV, $|\eta| <2.7$ and very loose identification
- No isolation requirements are made on electron and muon candidates.
- Photon candidates
  - $p_T > 20$GeV and tight identification and isolation criteria

- Particle flow (PFlow) jets. Reconstructed with anti-k_t algorithm
- Jets
  1. $p_T > 20$GeV, $|\eta| <4.5$
  2. *b*-jets. It is the identification (or "tagging") of jets originating from bottom quarks (b quarks). Some high-mass particles decay into bottom quarks. Higgs boson is expected to decay into bottom quarks more than any other particle given its mass.

Object and Event selection

To avoid double counting of energy deposits, the reconstructed objects are required to be separated

Remove	Keep	Matching criteria
electron	electron	shared inner detector track, electron with lower p_T removed
muon	electron	muon with calorimeter deposits and shared inner detector track
electron	muon	shared inner detector track
photon	electron	$\Delta R < 0.4$
photon	muon	$\Delta R < 0.4$
jet	electron	$\Delta R < 0.2$
electron	jet	$\Delta R < \min(0.4, 0.04 + 10\,\mathrm{GeV}/p_{\mathrm{T}}^{e})$
jet	muon	number of tracks < 3 and $\Delta R < 0.2$
muon	jet	$\Delta R < \min(0.4, 0.04 + 10\,\mathrm{GeV}/p_{\mathrm{T}}^{\mu})$
photon	jet	$\Delta R < 0.4$

- $\Delta R = \sqrt{\Delta y^2 + \Delta\phi^2}$ criterion

Object and Event selection

Object definitions and event cleaning

- Missing Transverse momentum E_T^{miss}
  1. Negative Vectorial sum of the transverse momenta and "soft term"
  2. There is regions other than the signal region. This is known as the control region and is used for the background measurement.
  3. One electron control regions: E_T^{miss} enrich enrich the contribution from multijet events with a fake electron: $S_{MET} = \frac{E_T^{miss}}{\sqrt{p_T^{j1}+p_T^{j2}+p_T^{e}}}$
- Several cleaning requirements are applied to suppress non-collision backgrounds

Object and Event selection

Signature from vector boson fusion VBF

- Two leading jets in opposite hemispheres of the detector are more forward than jets from non-VBF processes at scale $\sqrt{\hat{s}}$
- Large rapidity gap between the two leading jets.
- Events with three or four jets are considered as well but with additional requirements
- The centrality C_i of the third and forth highest p_T jet ($i = j3$ and $i = j4$). $C_i = exp(-\frac{4}{(\eta^{j1}-\eta^{j2})^2} \cdot (\eta^i - \frac{\eta^{j1}+\eta^{j2}}{2})^2)$
- Invariant mass m_{jj}: $m_i^{rel} = \frac{min(m_{j1,i}, m_{j2,i})}{m_{jj}}$
- Variables sensitive to the overall shape of the event

Object and Event selection

Event Selection in the signal region SR

- No lepton candidate, nor a photon
- The leading two jets are not back-to-back: $\Delta\phi_{jj} < 2.0$
- The leading and sub-leading jets $p_T > 80$GeV and $p_T > 50$GeV, respectively
- No more than one of the jets are *b*-tagged
- If $(i = j3)$ or $(i = j4)$ jet $\Rightarrow C_i < 0.6$ and $m_i^{rel} < 0.05$
- Event $E_T^{miss} > 200$ GeV, which strongly suppresses the multijet background. "Soft track" < 20 GeV

Object and Event selection

The selected events in the SR are split into eleven bins of different signal purity

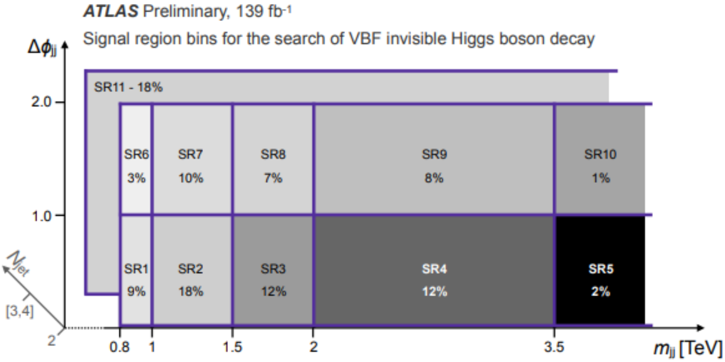

- Events from V+jets processes comprise about 95 of events that enter the SR.
- Large associated theoretical uncertainties.
- Used data driven technique that uses CRs with selected $Z\,(\to ll)$+jets and $W\,(\to l\nu)$+jets events
- The Z_{ll} CR is the same as the SR.

  but Lepton veto is replaced by two same opposite-sign "signal" leptons with $|m_{ll} - m_z| < 25$ GeV

  and Event with $E_T^{miss} < 70$ GeV
- W CR is the same as the SR.

  but Requires one "signal" lepton $p_T < 30$GeV

V+jets Background estimation

Z_{ll} CR with Z_{ee} (left) and $Z_{\mu\mu}$ (right)

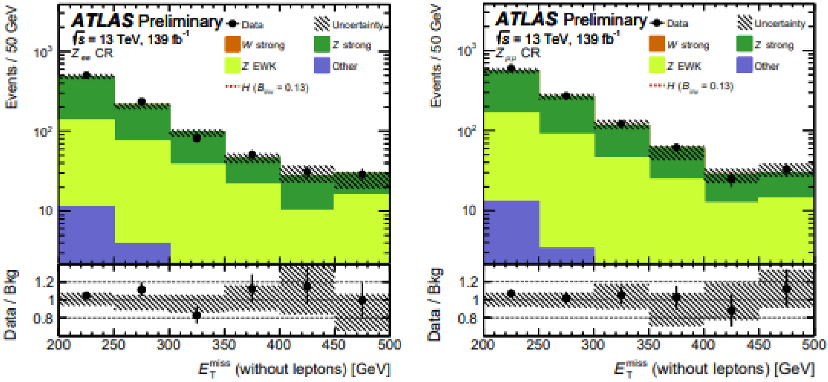

Multijet Background estimation

- Minor backgrounds arise from diboson and $t\bar{t}$ production taken from simulation, and (MJ) processes which are data driven.
- The signal selection is designed to heavily suppress events through the requirement of large E_T^{miss} and small $\Delta\phi_{jj}$
- Jet sample recorded by a set of single-jet triggers is used. And no lepton candidate
- Multijet background estimation apply a correction to account for the inefficiency of E_T^{miss} triggers used to collect the data.
- In MJ processes expected to have a contribution of events with fake electrons originating in which a jet is miss-identified as an isolated electron. Fulfil $S_{MET} > 4\sqrt{GEV}$

- The single-electron events that fail this S_{MET} selection define the "fake-e CR", which is enriched by fake electrons.

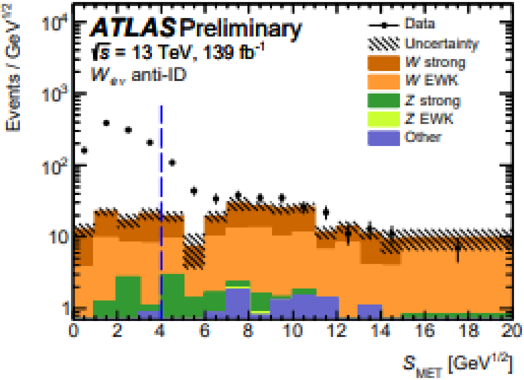

Systematic uncertainties

Theoretical Uncertainties

- Signal uncertainties: VBF and ggF Higgs boson production inclusive cross-sections and uncertainties are provided by the LHC Higgs working group. Evaluated by renormalisation and factorization scale variations.

Experimental Uncertainties

- Uncertainties on the luminosity. And on the trigger efficiencies.
- Uncertainties related to electrons, muons, jets, and the E_T^{miss}.
  - Electrons and muons: Uncertainties on the reconstruction and isolation efficiencies, energy scale and resolution.
  - Jets: Uncertainties on the energy scale and resolution, on the pile-up tagging efficiencies
  - Uncertainties on the reconstructed objects are propagated to the calculation of E_T^{miss}

Statistical model

- $B_i^{SR} = B_{Z,i}^{SR} + B_{W,i}^{SR} + B_{MJ,i}^{SR} + B_{other,i}^{SR}$
- Expected backgrounds after the signal selection by a simultaneous maximum likelihood fit of the background components to the data observed in all control and signal regions

$$
\begin{aligned}
\mathcal{L}(\mu, \vec{\beta}_Z, \vec{\beta}_W, \vec{n}_{\text{fake}}, \vec{\theta}) = \quad & \prod_i \mathcal{P}\left(N_i^{\text{SR}} \mid \beta_{Z,i} \cdot B_{Z,i}^{\text{SR,MC}} + \beta_{W,i} \cdot B_{W,i}^{\text{SR,MC}} + B_{\text{MJ},i}^{\text{SR}} + B_{\text{other},i}^{\text{SR,MC}} + \mu \cdot S_i^{\text{SR,MC}}\right) \\
& \prod_i \mathcal{P}\left(N_i^{Z\text{CR}} \mid \beta_{Z,i} \cdot B_{Z,i}^{Z\text{CR,MC}} + B_{\text{non-}Z,i}^{Z\text{CR}}\right) \\
& \prod_i \mathcal{P}\left(N_i^{W\mu\nu\text{CR}} \mid \beta_{W,i} \cdot B_{W,i}^{W\mu\nu\text{CR,MC}} + B_{\text{non-}W,i}^{W\mu\nu\text{CR,MC}}\right) \\
& \prod_i \mathcal{P}\left(N_i^{We\nu\text{CR}} \mid \beta_{W,i} \cdot B_{W,i}^{We\nu\text{CR,MC}} + B_{\text{non-}W,i}^{We\nu\text{CR,MC}} + R_{S,i} \cdot n_{\text{fake},i}\right) \\
& \prod_i \mathcal{P}\left(N_i^{\text{fake-}e\text{ CR}} \mid \beta_{W,i} \cdot B_{W,i}^{\text{fake-}e\text{ CR,MC}} + B_{\text{non-}W,i}^{\text{fake-}e\text{ CR,MC}} + n_{\text{fake},i}\right) \\
& \prod_j \mathcal{G}\left(0|\theta_j\right),
\end{aligned}
$$

Results

- Expected backgrounds in the inclusive signal and control regions after the likelihood fit

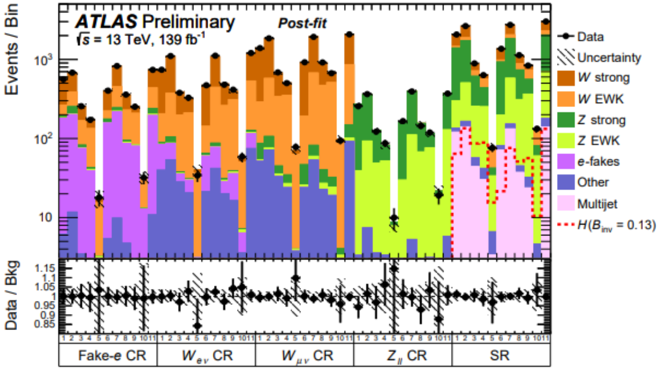

- m_{jj} and $\Delta\phi_{jj}$ distributions

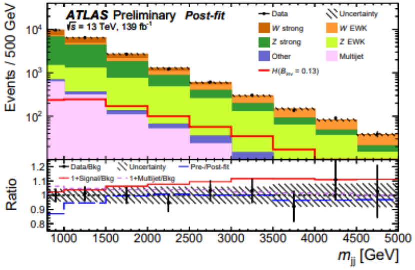

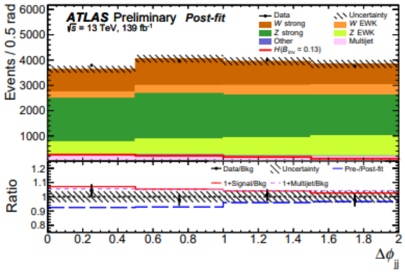

Results

- Impact of the systematic uncertainties on the upper limit on B_{in}

Source	Δ [%]
Jet energy scale	1.8
Jet energy resolution	5.5
Lepton	4.6
Other	1.9
Multijet	7.0
V+jets theory	1.6
Signal theory	1.0
MC stats.	7.9
Data stats.	17.3

- Upper limits on the spin-independent WIMP–nucleon cross section of B_{inv} at 90% CL vs. m_{wimp}

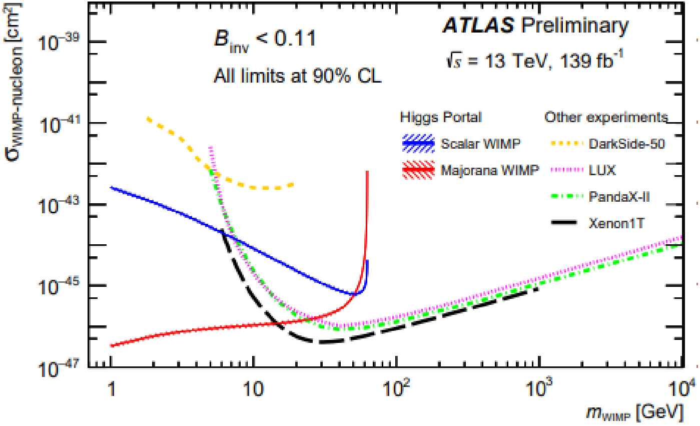

Results

- Upper limit on cross section times branching ratio to invisible particles

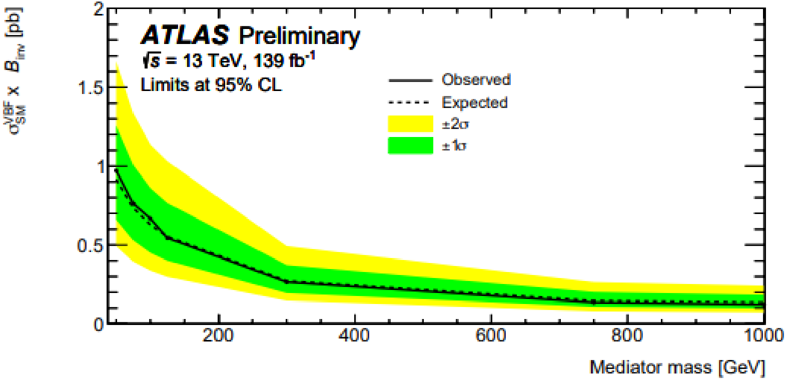

THANK YOU SO MUCH FOR YOUR ATTENTION